Original Article

CYP3A4 overexpression enhances the cytotoxicity of the antitumor triazoloacridinone derivative C-1305 in CHO cells

Ewa AUGUSTIN*, Barbara BOROWA-MAZGAJ, Agnieszka KIKULSKA, Milena KORDALEWSKA, Monika PAWŁOWSKA

Department of Pharmaceutical Technology and Biochemistry, Chemical Faculty, Gdańsk University of Technology, Narutowicza Str 11/12, 80–233 Gdańsk, Poland

Aim: To examine how the higher expression level of CYP3A4 isoenzyme influenced the cytotoxicity of the antitumor triazoloacridinone derivative C-1305 in Chinese hamster ovary (CHO) cells.
Methods: Three CHO cell lines were examined: wild-type CHO cells; CHO-HR cells with overexpression of human cytochrome P450 reductase (CPR); and CHO-HR-3A4 cells with coexpression of human CYP3A4 and CPR. Cellular responses caused by C-1305 were monitored using DAPI staining, cell cycle analysis, phosphatydilserine externalization analysis and SA-β-galactosidase expression analysis. Cell viability was assessed with simultaneous FDA and PI staining.
Results: Treatment with C-1305 for 72 h exhibited different levels of cytotoxicity in the 3 cell lines, and the values of IC80 in CHO, CHO-HR and CHO-HR-3A4 cells were 0.087±0.005, 0.032±0.0001, and 0.064±0.0095 µmol/L, respectively. The cell cycle analysis revealed that both CHO and CHO-HR cells underwent transient G_2/M arrest, whereas CHO-HR-3A4 cells did not accumulate in this phase. Prolonged exposure up to 120 h caused time-dependent increase in the sub-G_1 fraction in all the 3 cell lines. Treatment with C-1305 caused cell death through apoptosis and necrosis. However, these processes were more pronounced in the transfected CHO cells than in the wild-type cells. The cells surviving after C-1305 exposure underwent senescence.
Conclusion: CYP3A4 overexpression potently enhances the cellular responses (apoptosis, necrosis and senescence) caused by C-1305 in CHO cells.

Keywords: apoptosis; triazoloacridinones; C-1305; CHO cells; CYP3A4; cellular response; apoptosis; necrosis; senescence

Introduction

Differences in the expression levels of drug-metabolizing enzymes, particularly cytochrome P450, can affect the cellular response to anticancer drugs for at least two reasons: first, the patients are characterized by the individual levels of selected cytochrome P450 isoenzymes, and second, tumor tissues very often express different levels of metabolizing enzymes (such as CYP1B1 and CYP3A4) that are higher or lower compared with the adjacent normal tissues in which the tumors have developed[1, 2]. Consequently, differences in the levels of CYP3A4 can change the effectiveness of antitumor agents. Therefore, cellular model systems that overexpress cytochrome P450 proteins have been developed to explore the influence of enzyme levels on the cellular and molecular mechanisms of action of potential drugs and drugs that are currently used therapeutically.

The level of functional CYP expression largely depends on the host cells[3]. Moreover, the activity of the CYP3A4 enzyme expressed in several stable mammalian cell lines is much lower than the activity of this enzyme in human liver cells. The low expression level of recombinant CYP3A4 may be due to the low copy number of the cDNA used to express it. In addition, the low activity is caused by the low level of P450 reductase in the host cells[4]. To achieve high levels of cellular CYP3A4 expression, Thomas FRIEDBERG and coworkers employed gene amplification of the CYP3A4 cDNA in CHO cells followed by transfection of the P450 reductase cDNA. They obtained a cell line with a high level of recombinant human CYP3A4 that coexpressed P450 reductase and CYP3A4[5].

We used a CHO model system to elucidate the influence of cytochrome P450 enzymes on the overall cellular response induced by the triazoloacridinone derivative C-1305.

C-1305 (5-dimethylaminopropylamino-8-hydroxytriazolo-acridinone) is a potent antitumor compound that was devel-

oped at the Gdańsk University of Technology[6] (Figure 1A). This drug is the most active derivative among the triazolo-acridinones and was selected for extended preclinical trials. C-1305 exhibits significant cytotoxic activity *in vitro* and potent antitumor activity towards a wide range of experimental tumors in mice (particularly leukemias, colon cancers and melanomas)[7]. This drug is a DNA topoisomerase II inhibitor that stabilizes covalent complexes between DNA and the topoisomerase enzyme[8]. Compared to classic topoisomerase II inhibitors, such as amsacrine, C-1305 produces only low levels of cleavable complexes. Moreover, C-1305 strongly affected the proliferation of cells lacking PARP-1, in contrast to other topoisomerase II inhibitors[9]. Interestingly, the pharmacological inhibition of PARP-1 with NU1025 sensitizes HeLa cells to C-1305[10].
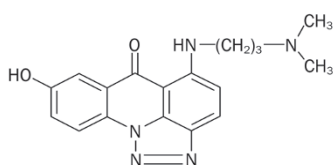

Figure 1. The chemical structure of C-1305, 5-dimethylaminopropylamino-8-hydroxytriazoloacridinone.

C-1305 possesses higher affinity to GC than AT sequences in DNA[11], and the zwitterionic form of C-1305 intercalates within guanine triplets, resulting in the widening of both major and minor DNA grooves and alignment of the triazole rings with the N7 atoms of guanine. The structural perturbation induced by C-1305 plays an important role in the biological activity of this drug[11]. It has also been postulated that the cytotoxic action of C-1305 is affected by its ability to induce interstrand covalent DNA crosslinks in tumor cells after metabolic activation[12].

At the cellular level, C-1305 induces G_2/M arrest and subsequent apoptosis in human leukemia cells[13], which confirms that C-1305 could be considered a promising new antitumor agent.

Studies on the metabolism of C-1305 showed that the flavin-containing monooxygenases FMO-1 and FMO-3 are responsible for its biotransformation in liver microsomes and human hepatoma cells. Moreover, C-1305 is an inhibitor of the cytochrome P450 isoenzymes CYP1A2 and CYP3A4[14].

In this work, we evaluated whether the overexpression of the CYP3A4 isoenzyme influences cell cycle progression and the overall cellular response induced by C-1305 in the Chinese hamster ovary model system. Our results contribute to knowledge of the pharmacological properties of C-1305, which can be useful for predicting the effectiveness of therapies designed for individual patients and selectively targeting cancer cells.

Materials and methods
Chemicals and reagents
C-1305 was synthesized in the Department of Pharmaceuti-cal Technology and Biochemistry as described previously[6]. A stock solution of C-1305 was prepared in 50% ethanol and stored at -20 °C until use. The Annexin-V-Fluos Staining Kit was obtained from Roche Diagnostics (Manheim, Germany). RNase A, DAPI, PI, FDA, methotrexate, G-418, SA-β-gal, and all other reagents were obtained from Sigma-Aldrich (St Louis, MO, USA). The FITC-conjugated Monoclonal Active Caspase-3 Antibody Apoptosis Kit was purchased from BD Pharmingen (San Diego, CA, USA). All mammalian cell culture reagents were purchased from GIBCO-BRL Life Technologies (Paisley, UK).

Cell lines and culture
Three Chinese hamster ovary cell lines were used in this study: CHO (wild-type), CHO-HR (overexpressing human P450 reductase, the donor of reducing equivalents for P450), and CHO-HR-3A4 (coexpressing human P450 reductase and CYP3A4). These cell lines[5] were obtained by Dr Thomas FRIEDBERG from the Biomedical Research Centre, Dundee, Scotland and were kindly provided for these studies. CHO and CHO-HR cells were grown in DMEM (Dulbecco's modified Eagle's medium, 4.5 g/L glucose) supplemented with 10% fetal bovine serum, antibiotics (100 µg/mL streptomycin, 100 IU/mL penicillin), and 1 IU/mL HAT (hypoxanthine and thymidine) under a 5% CO_2 atmosphere at 37 °C. To maintain P450 reductase expression, the media were additionally supplemented with G418-sulfate (400 µg/mL) to exert selection pressure. CHO-HR-3A4 cells were grown in MEM alpha (minimum essential medium) supplemented with 10% dialyzed fetal bovine serum and antibiotics (100 µg/mL streptomycin, 100 IU/mL penicillin). To maintain CYP and P450 reductase expression, the media were additionally supplemented with G418-sulfate (400 µg/mL) and methotrexate (0.3 µmol/L). Under these growth conditions, the cell-doubling time was approximately 18 h for CHO cells, 22 h for CHO-HR cells and 30 h for CHO-HR-3A4 cells. All of the experiments were performed with cells in the exponential phase of growth. Moreover, in all of the experiments concerning the influence of higher expression levels of the CYP3A4 isoenzyme on cell cycle progression and the cellular response following C-1305 treatment, methotrexate was not added.

Growth inhibition assay
Cell growth inhibition was determined by cell counting using a Beckman Coulter Z1. Cells in the exponential growth phase (2×10^4 cells for CHO and CHO-HR cells; 3.5×10^4 cells for CHO-HR-3A4 cells) were seeded in 24-well microculture plates and treated with various C-1305 concentrations ranging from 0.0001 µmol/L to 10 µmol/L for 72 h. A dose-response curve was plotted and used to calculate the drug concentration required to inhibit cell growth by 50% and 80% (IC_{50} and IC_{80}, respectively).

Cell cycle analysis
Cells were stained with propidium iodide (PI) and monitored using a FACScan (Becton Dickinson, San Jose, CA, USA) as

described previously[13].

Assessment of cell morphology

The nuclear morphology of the cells was examined under a fluorescence microscope (OLYMPUS BX60, 40×objective) after staining with 4′,6-diaminidino-2-phenylindole (DAPI). Briefly, after drug incubation, the cells (1.5×10^6) were spun onto microscope slides, fixed in a methanol:acetic acid solution (3:1) for 15 min and stained with DAPI (1 µg/mL) for 5 min. Cells were identified as apoptotic based on the presence of condensed, fragmented chromatin. Enlarged cells containing multiple nuclei were considered typical for mitotic catastrophe.

Externalization of phosphatidylserine

An Annexin V-FITC binding assay was performed using the Annexin-V-Fluos Staining kit (Roche Diagnostics, Mannheim, Germany) according to the manufacturer's instructions. Briefly, after drug incubation, the cells (1.5×10^6) were trypsinized, rinsed with PBS, pelleted and resuspended in 50 µL of Annexin V-FITC diluted in binding buffer containing PI. The cells were incubated for 15 min at room temperature in the dark, diluted with 350 µL of binding buffer and analyzed by flow cytometry within 1 h. Flow cytometric analyses were performed using a FACScan cytometer (Becton Dickinson, San Jose, CA, USA). At least 1×10^4 cells were collected, and data analysis was performed using WinMDI software (J Trotter, Scripps Research Institute, San Diego, CA, USA).

Caspase-3 activity

The level of activated caspase-3 was determined using the Active Caspase-3 Apoptosis kit (BD Pharmingen, San Diego, USA) according to the manufacturer's instructions. The cells (1×10^6) were stained with FITC-conjugated anti-active caspase-3 antibody and analyzed by flow cytometry (FACScan cytometer, Becton Dickinson, San Jose, CA, USA). The data analyses were performed as noted below.

Double-staining with FDA and PI

To assess the number of dead cells following C-1305 treatment, simultaneous double staining with fluorescein diacetate (FDA) and propidium iodide (PI) was performed. Briefly, 2×10^6 untreated (control) or C-1305-treated CHO cells were washed twice with PBS, resuspended in an FDA/PI solution (stocks: 1 mg/mL FDA and 1 mg/mL PI) diluted in PBS. The cells were stained for 15 min at room temperature and then applied to a microscope slide and examined under a fluorescence microscope (Olympus, BX60, 20×objective).

Beta-galactosidase staining

Senescence-associated (SA) beta-galactosidase histochemical staining in the CHO cells was performed after exposure to C-1305 as described by Dimri *et al*[15]. Following C-1305-treatment, the cells (1×10^5) were washed twice with PBS and fixed with 2% formaldehyde and 0.2% glutaraldehyde in PBS for 5 min. The cells were then washed again with PBS

and stained with a solution of 1 mg/mL 5-bromo-4-chloro-3-indolyl-β-*D*-galactosidase in dimethylformamide (20 mg/mL stock), 5 mmol/L potassium ferrocyanide, 5 mmol/L potassium ferricyanide, 150 mmol/L NaCl, 40 mmol/L citric acid/sodium phosphate, pH 6.0, and 2 mmol/L $MgCl_2$. Following overnight incubation at 37 °C, the cells were washed twice with PBS and representative fields were photographed under a light microscope (Olympus BX60, 20×objective).

Statistical analysis

All of the assays were performed in triplicate. The data were expressed as the mean±SD, or a single experiment was presented as a representative of the three experiments. Values were compared with Student's unpaired *t*-test, and the difference was considered significant at $P < 0.05$. Analysis of variance (one-way ANOVA) was carried out using GraphPad Prism (GraphPad Software, Inc, San Diego, CA, USA).

Results

Inhibition of CHO cells proliferation

Significant dose-dependent inhibition of cell proliferation was observed in CHO cells after treatment with C-1305 at 0.0001–10 µmol/L for 72 h (data not shown). The three studied CHO cell lines showed different sensitivities to C-1305 (Table 1). The estimated concentration required to inhibit cell growth by 80% (IC_{80}) demonstrated that CHO-HR cells overexpressing human P450 reductase exhibited the highest sensitivity to C-1305, whereas CHO wild-type cells were the least sensitive to this drug (IC_{80} values of 0.032 µmol/L and 0.087 µmol/L, respectively). In turn, CHO-HR-3A4 cells coexpressing human P450 reductase and CYP3A4 exhibited an intermediate sensitivity to C-1305 (IC_{80} of 0.064 µmol/L). The calculated EC_{80} values were used in all of the subsequent experiments regarding the cellular response of CHO cells to C-1305 treatment.

Table 1. Growth inhibition of C-1305 against CHO cell lines.

Cell line	IC_{50} (µmol/L)*	IC_{80} (µmol/L)*
CHO	0.032±0.006	0.087±0.005
CHO-HR	0.012±0.0008[b]	0.032±0.0001[c]
CHO-HR-3A4	0.0099±0.0041[b]	0.064±0.0095[bf]

* Each value represented the mean±SD of three independent experiments. [b]$P < 0.05$, [c]$P < 0.01$ *vs* CHO wild type, [f]$P < 0.01$ *vs* CHO-HR.

Cell cycle changes following C-1305 treatment

The effect of C-1305 on cell cycle progression in CHO cells was determined by flow cytometry following drug treatment for 24–120 h. Analysis of nuclear DNA distribution revealed that C-1305 induced a time-dependent increase in the population of hypoploid cells (<2N DNA content, sub-G_1 cells), representing cells undergoing apoptosis (Figure 2). The fraction of sub-G_1 cells increased from 1.8% in control (non-treated) cells
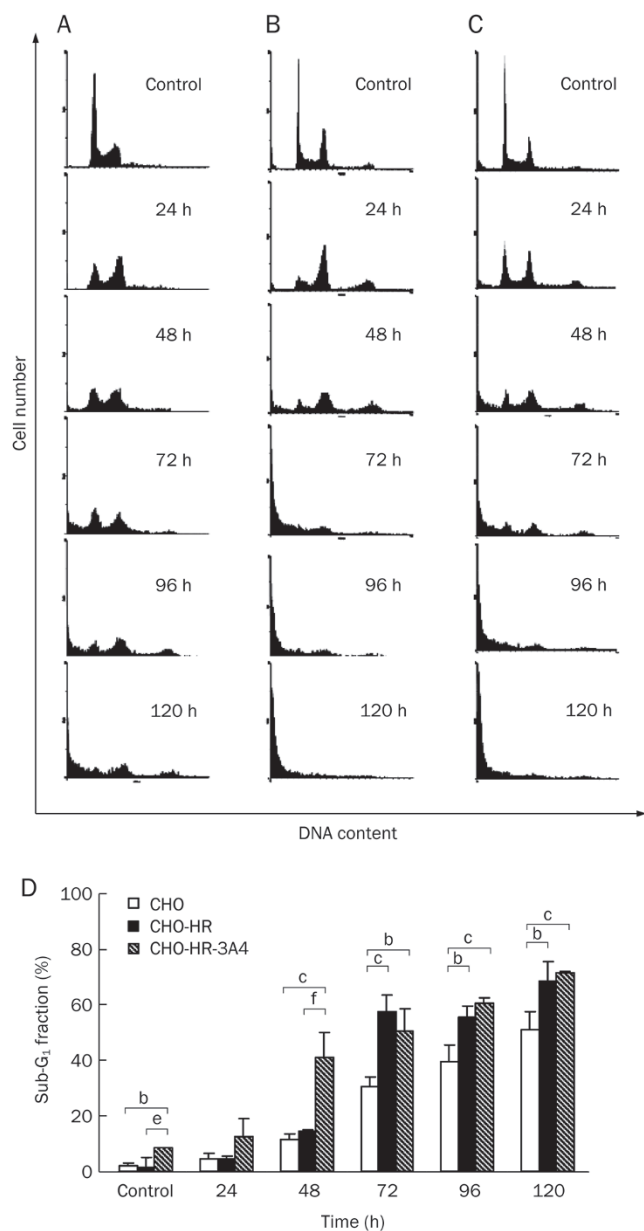
Figure 2. Effect of C-1305 on DNA distribution in CHO (A), CHO-HR (B) and CHO-HR-3A4 (C) cells after the treatment times indicated. The cells were fixed in ethanol, stained with PI and their DNA content was measured using a FACScan. Representative histograms of three independent experiments are shown. (D) The percentage of wild-type and transfected CHO cells in the sub-G_1 fraction (considered as apoptotic) treated with C-1305 at the IC_{80} for the times indicated. The percentages were calculated by deconvolution of the DNA content histograms. Statistical significance was determined by student's *t*-test. Mean±SD. *n*=3. [b]$P<0.05$, [c]$P<0.01$ *vs* CHO cells. [e]$P<0.05$, [f]$P<0.01$ *vs* CHO+HR cells.

to 50% in wild-type CHO cells treated with C-1305 for 120 h. The sub-G_1 fraction was higher in CHO-HR cells overexpressing P450 reductase and increased from 1.5% in control (nontreated) cells to 69% in cells treated with C-1305 for 120 h. DNA degradation was most prominent in CHO-HR-3A4 cells

coexpressing P450 reductase and the CYP3A4 isoenzyme, and the sub-G_1 fraction represented 72% of the total population following 120 h of drug treatment (Figure 2D). Longer incubation times for up to 192 h resulted in proportional increases in the sub-G_1 fraction in the three studied CHO cell lines (data not shown). In addition, accumulation of CHO and CHO-HR cells in the G_2/M compartment was detectable at 24 h after C-1305 treatment (Figures 2A and 2B). Starting at 48 h, the reduction in G_2/M arrest was associated with a gradual increase in the sub-G_1 DNA content, which is indicative of apoptosis. This cell cycle arrest did not appear in CHO-HR-3A4 cells following C-1305 treatment (Figure 2C). Moreover, the number of CHO-HR-3A4 cells in all phases was markedly reduced, and there was a concomitant increase in the population of cells with <2N DNA content.

Assessment of nuclear morphology by DAPI staining

To further explore the effect of the triazoloacridinone C-1305 on the types of cellular responses in CHO cells, the changes in nuclear morphology following exposure to the IC_{80} drug concentration were assessed by DAPI staining. As shown in Figures 3A, 3B, and 3C, untreated CHO wild-type and transfected cells demonstrated unchanged morphology with homogenously distributed chromatin within their nuclei. Beginning at 24 h of C-1305 treatment, CHO-HR and CHO-HR-3A4 cells displayed condensed and fragmented nuclei, which are characteristic of apoptotic cells. Wild-type CHO cells presented features typical for apoptosis beginning at 72 h of drug treatment. Additionally, after prolonged drug incubation (120 h and longer), a small population of CHO cells (wild-type and transfected) presented morphological features of mitotic death, *ie*, the nuclei became significantly larger and some of the cells contained several nuclei (micronuclei). Moreover, after 6 or more days of C-1305 treatment, the transfected cells (CHO-HR and CHO-HR-3A4) began to detach from the culture plates, which may suggest that this population underwent necrosis.

Annexin V/PI dual staining to detect plasma membrane integrity

To confirm that apoptotic cell death is the principal cellular response of CHO cells to C-1305 treatment, Annexin V/PI staining was performed. During apoptosis, cells lose their asymmetry, and phosphatidylserine (PS) translocates from the cytoplasmic face on the plasma membrane to the cell surface and can interact with Annexin V, which has a high affinity for PS. In contrast, PI can only enter cells after loss of membrane integrity. Thus, dual staining with Annexin V and PI can be used to classify cells as early apoptotic (AV[+]/PI[-]), late apoptotic (AV[+]/PI[+]) or necrotic (AV[-]/PI^{+}) cells. The flow cytometry results showed time-dependent increases in apoptotic CHO cells after treatment with the triazoloacridinone C-1305 at the IC_{80} (Figures 4A, 4B, and 4C). In the case of wild-type CHO cells, the populations of early (AV[+]/PI[-]) and late apoptotic (AV[+]/PI^{+}) cells were minimal at 24 h (5%) and increased to approximately 32% after 120 h (Figure 4D). Compared to wild-type CHO cells, the population of apoptotic CHO-HR cells (overexpressing P450 reductase) was higher and reached
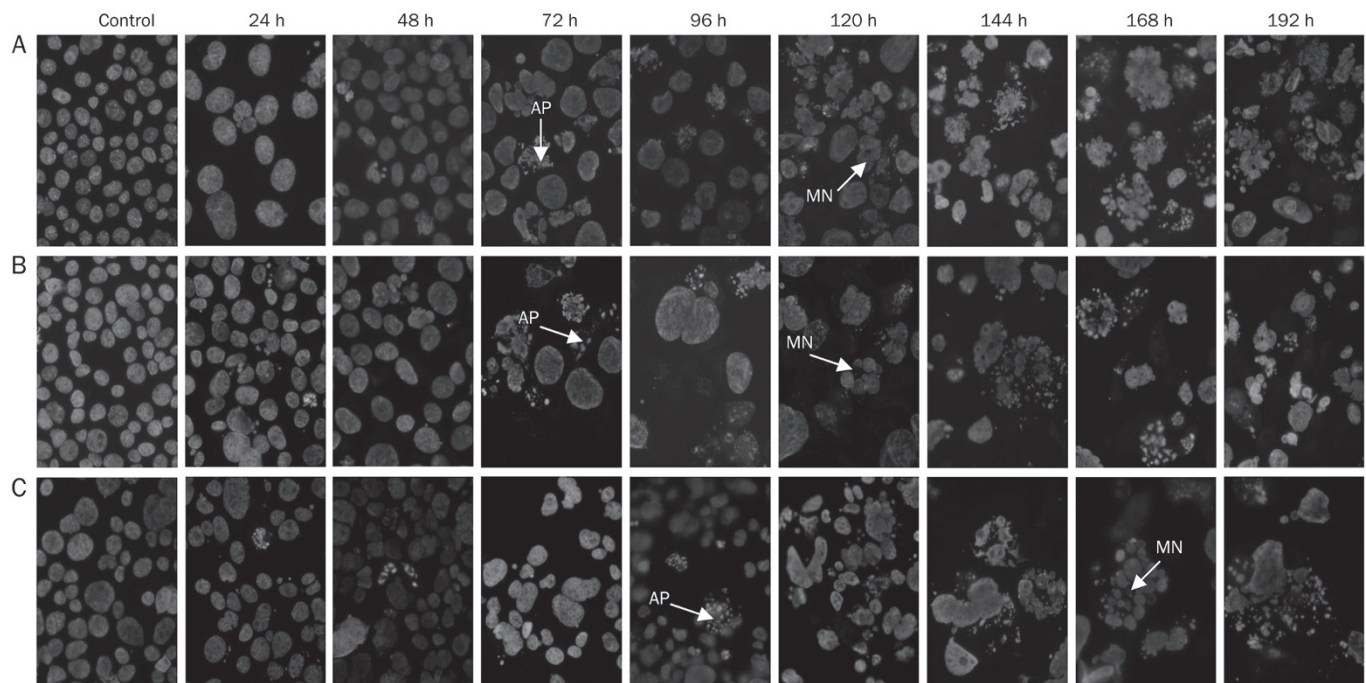
Figure 3. Changes in the nuclear morphology of non-treated (control) and C-1305-treated CHO cells. Representative pictures of CHO (A), CHO-HR (B) and CHO-HR-3A4 (C) cells stained with DAPI and examined under a fluorescence microscope (magnification 400×). Cells with condensed, intensely stained fragmented chromatin are typical of apoptosis (arrow AP). Enlarged, multinucleated cells are characteristic for mitotic catastrophe (arrow MN).

approximately 48% after 120 h of drug treatment (Figure 4D). The number of apoptotic CHO-HR-3A4 cells (coexpressing P450 reductase and CYP3A4) was approximately 37% after C-1305 treatment for 120 h (Figure 4D). Approximately 16% of the CHO and 19% of the CHO-HR cells treated with C-1305 for 96 h underwent necrosis, and these populations were slightly decreased following 120 h of incubation (Figure 4E). The population of necrotic CHO-HR-3A4 cells was lower and reached approximately 7% after 96–120 h of drug treatment (Figure 4E).

C-1305 induces apoptosis in a caspase-dependent manner
Caspases are cell-death proteases that play a significant role in both the initiation and execution of apoptotic programs in diverse species. Caspase-3 is very important for the execution stage of apoptosis[16]. Accordingly, exposure of CHO cells to C-1305 resulted in a time-dependent increase of activated caspase-3 as measured by flow cytometry (Figure 5). In wild-type CHO and CHO-HR cells after 120 h of treatment, the percentage of cells expressing active caspase-3 reached approximately 34%–37%. Compared to these cells, the percentage of CHO-HR-3A4 cells expressing active caspase-3 after C-1305 treatment was significantly higher ($P<0.05$); after 120 h this percentage reached approximately 66% (Figure 5D). These results suggest that C-1305-induced apoptosis in Chinese hamster ovary cells was mediated by caspase-3 activation, which was more prominent in transfected CHO cells than in wild-type cells.

Determination of cell viability
To directly assess the number of dead CHO cells following C-1305 exposure, untreated cells and cells treated with C-1305 at the IC_{80} for 24–192 h were labeled with FDA and PI. FDA is a nonpolar ester that passes through cell membranes and is hydrolyzed by intracellular esterases to produce fluorescein. The fluorescein, a polar compound that passes slowly through a living membrane, accumulates inside the cell and exhibits a green fluorescence. While FDA stains viable cells, injured and dead cells are stained using PI, which passes through damaged cell membranes, intercalates into DNA and emits a red fluorescence[17]. As depicted in Figures 6A, 6B, and 6C, a time-dependent increase in PI-stained cells was observed following C-1305 treatment. After 72 h of drug treatment, the fraction of dead cells that produced red fluorescence reached 14% in wild-type CHO cells, 24% in CHO-HR cells and 36% in CHO-HR-3A4 cells (Figure 6D). After prolonged drug incubation (192 h), the number of PI-positive cells in the different groups reached 65% (CHO cells), 71% (CHO-HR cells) and 93% (CHO-HR-3A4 cells).

Induction of cellular senescence
Exposure of CHO cells to C-1305 resulted principally in apoptosis and, to a lesser extent, necrosis. However, a small population of a surviving CHO cells could still be detected. Therefore, we investigated whether cells that survived after C-1305 treatment underwent senescence. Most senescent cells show a characteristic phenotype defined by the development
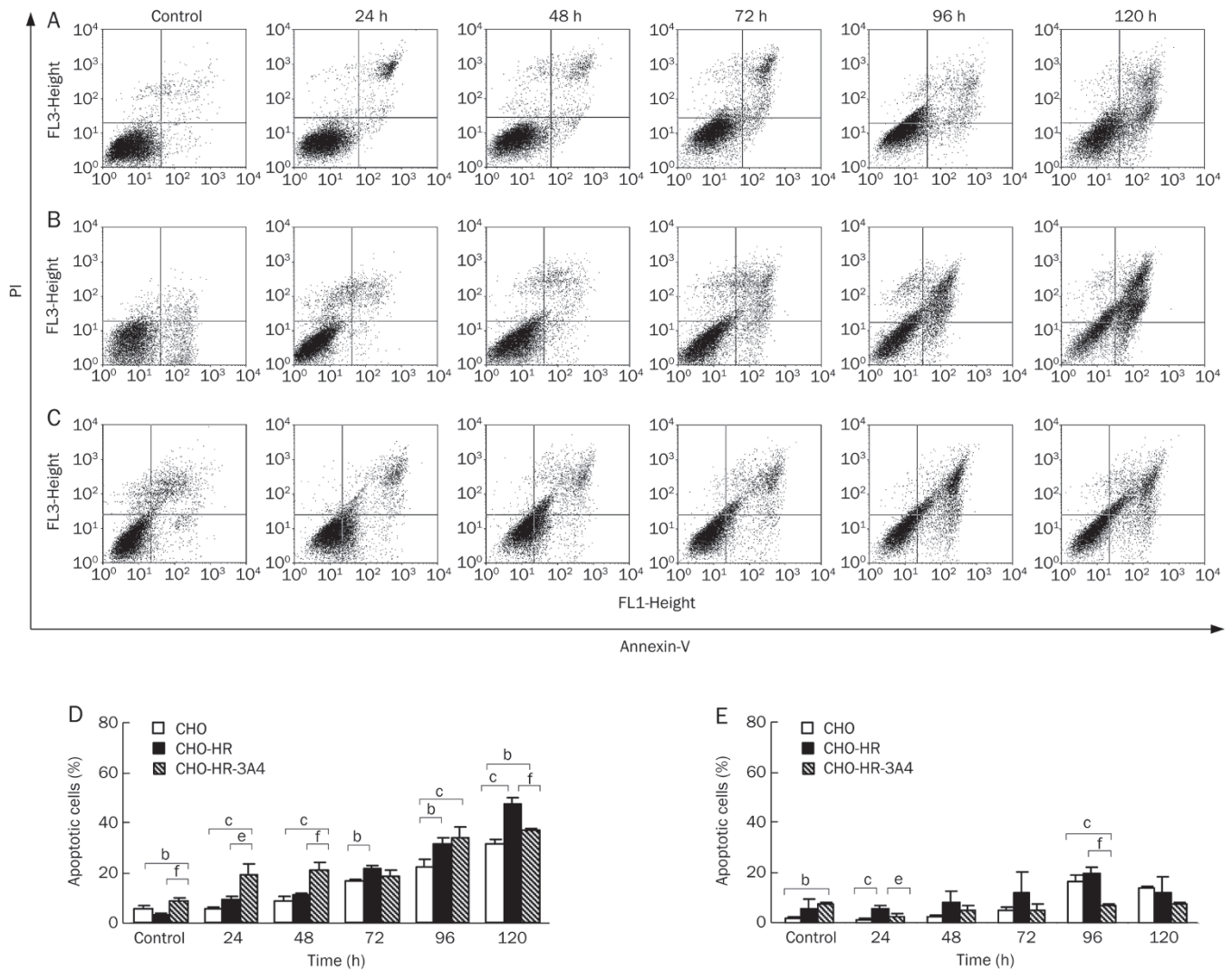
Figure 4. Flow cytometry analysis of membrane alterations in CHO (A), CHO-HR (B) and CHO-HR-3A4 (C) cells treated with C-1305. Cells in the bottom left quadrant are viable (Annexin V$^-$/PI$^-$); cells in the bottom right quadrant are in early apoptosis (Annexin V$^+$/PI$^-$); cells in the top right quadrant are in late apoptosis or in secondary necrosis (Annexin V$^+$/PI$^+$); and cells in the top left quadrant are in late necrosis (Annexin V$^-$/PI$^+$). Data are representative of three independent experiments. The percentages of apoptotic (D) and necrotic (E) CHO, CHO-HR, and CHO-HR-3A4 cells following C-1305 treatment at the IC$_{80}$ are given. Statistical significance was determined using student's *t*-test. Mean±SD. *n*=3. [b]$P<0.05$, [c]$P<0.01$ *vs* CHO cells. [e]$P<0.05$, [f]$P<0.01$ *vs* CHO-HR cells.

of an enlarged and flattened morphology accompanied by increased granularity and the detection of senescence-associated β-galactosidase (SA-β-gal) activity at pH 6.0[18]. In the three CHO cell lines studied, increased β-galactosidase staining relative to the control was observed 72 h after treatment with C-1305 (Figure 7). The number of SA-β-gal-positive cells continued to increase, and after 192 h of C-1305 exposure, the entire population of wild-type CHO and CHO-HR cells exhibited β-galactosidase staining (Figures 7A and 7B, respectively). Together with increased β-galactosidase staining, these cells had an enlarged and flattened morphology, which is typical for senescent cells. Compared to CHO and CHO-HR cells, in CHO-HR-3A4 cells the senescence process was observed after up to 120 h of C-1305 treatment, and beginning at 144 h of

drug exposure, only a few cells presented features typical for senescence (Figure 7C). This observation is consistent with the fact that after prolonged drug incubation (192 h), 93% of CHO-HR-3A4 cells were dead and were PI-positive (Figure 6D).

Discussion

Metabolism of cancer therapeutics by the host organism is one of the most important determinants of their pharmacokinetics and disposition. In most cases, metabolism leads to the inactivation of drugs. However, the metabolic transformation of xenobiotics can also sometimes generate an active metabolite that can be responsible for the final pharmacological response. In some cases, metabolic transformation can produce reactive or toxic metabolites with potential toxicological implications.
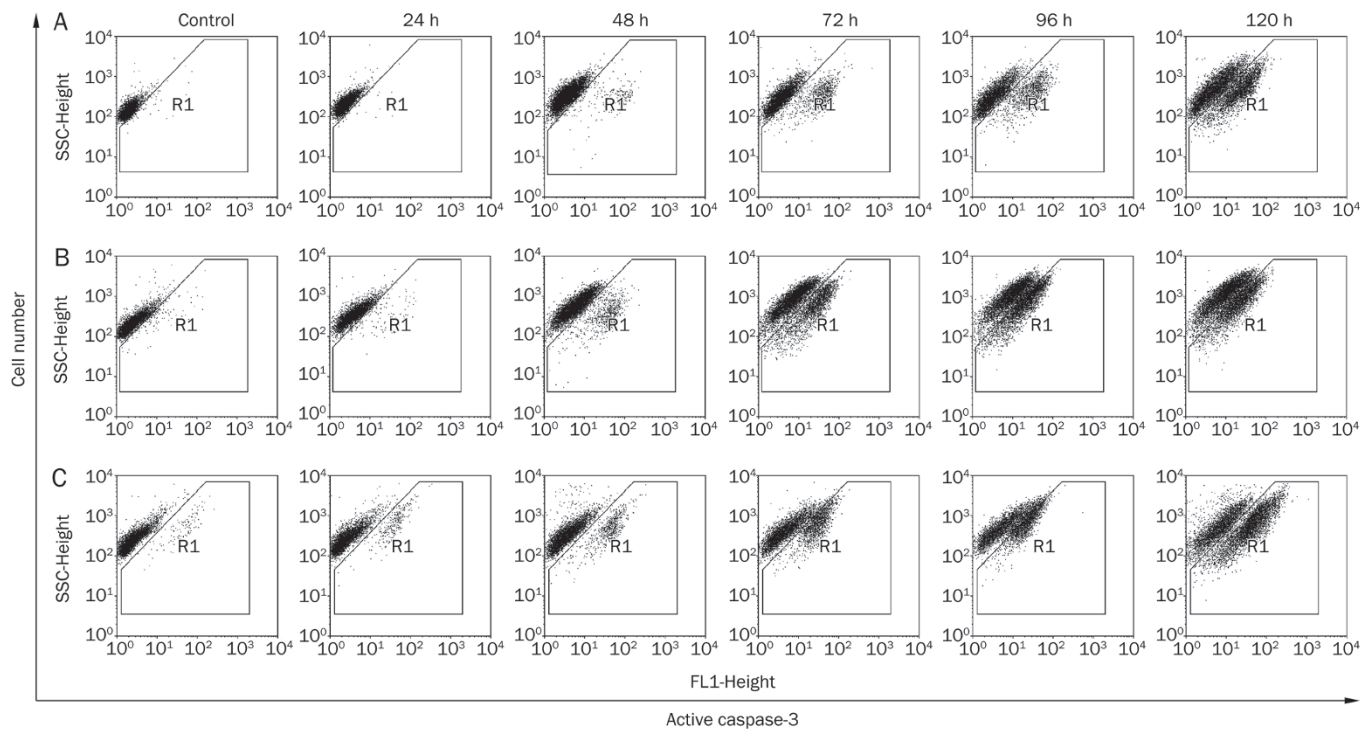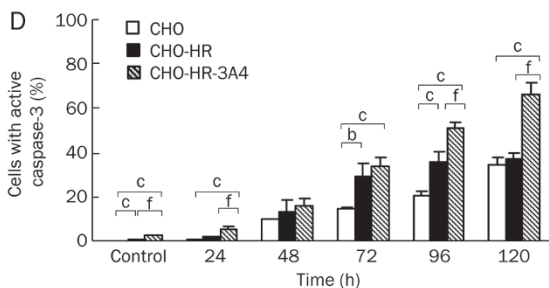
Figure 5. Assessment of caspase-3 activity in CHO cells treated with C-1305 for the times indicated. Upper panel: Representative bivariate flow cytometry histograms of caspase-3 activation in CHO (A), CHO-HR (B) and CHO-HR-3A4 (C) cells following treatment with C-1305 at the IC_{80}. Lower panel: Quantitation of the percentage of caspase-3-positive cells based on flow cytometry analysis. Statistical significance was determined using student's *t*-test. Mean±SD. *n*=3. [b]$P<0.05$, [c]$P<0.01$ *vs* CHO cells. [f]$P<0.01$ *vs* CHO-HR cells.

Therefore, knowledge about the metabolism of a new chemotherapeutic may be helpful in the prediction of drug-drug interactions with coadministered drugs due to the inhibition and/or the induction of drug metabolism pathways[19].

Several forms of cytochrome P450 are thought to have an important role in tumor development because they can metabolize many potential carcinogens and mutagens[20–22]. Moreover, cytochrome P450 activity may influence the response of established tumors to anticancer drugs because several chemotherapeutic agents can be either activated or detoxified by this enzyme system[21, 23, 24]. It has also been shown that the presence of individual forms of cytochrome P450 in different types of tumors (breast, lung, colon, head and neck) can influence the response of tumors to anticancer agents[25–27]. Moreover, the differential expression of cytochrome P450 enzymes within the tumor microenvironment compared with the surrounding normal tissue can also affect the tumor response to chemotherapeutics.

There is increasing evidence indicating that different expression levels of CYPs may modify the final biological response (cell death) induced by anticancer compounds[28, 29]. Moreover, the overexpression of P450 isoenzymes can enhance or

inhibit apoptosis induced by chemotherapeutics agents[30–32]. To explore the influence of cytochrome P450 isoenzymes on the biological responses induced by potential anticancer drugs and those used therapeutically, several expression systems for cytochrome P450 proteins in mammalian cells have been designed[33, 34]. One of them is the CHO model system designed by Thomas FRIEDBERG[5], which comprises three cell lines: wild-type CHO cells and two transfected cell lines, CHO-HR (overexpressing human P450 reductase) and CHO-HR-3A4 (coexpressing human P450 reductase and CYP3A4). In our work, these cell lines were used to examine whether CYP3A4 overexpression affects cell cycle progression and cell death following C-1305 treatment.

Studies of its cytotoxic activity demonstrated that three Chinese hamster ovary cell lines exhibited different sensitivities to C-1305, which was expressed as the IC_{80}. The transfected CHO cells were more sensitive to C-1305 than wild-type cells, and the cells that overexpressed only human P450 reductase (CHO-HR cells) were the most sensitive. The concentrations required to inhibit cell growth by 80% (IC_{80}) were as follows: 0.03 µmol/L for CHO-HR cells, 0.06 µmol/L for CHO-HR-3A4 cells and 0.09 µmol/L for wild-type CHO cells (Figure 1B).
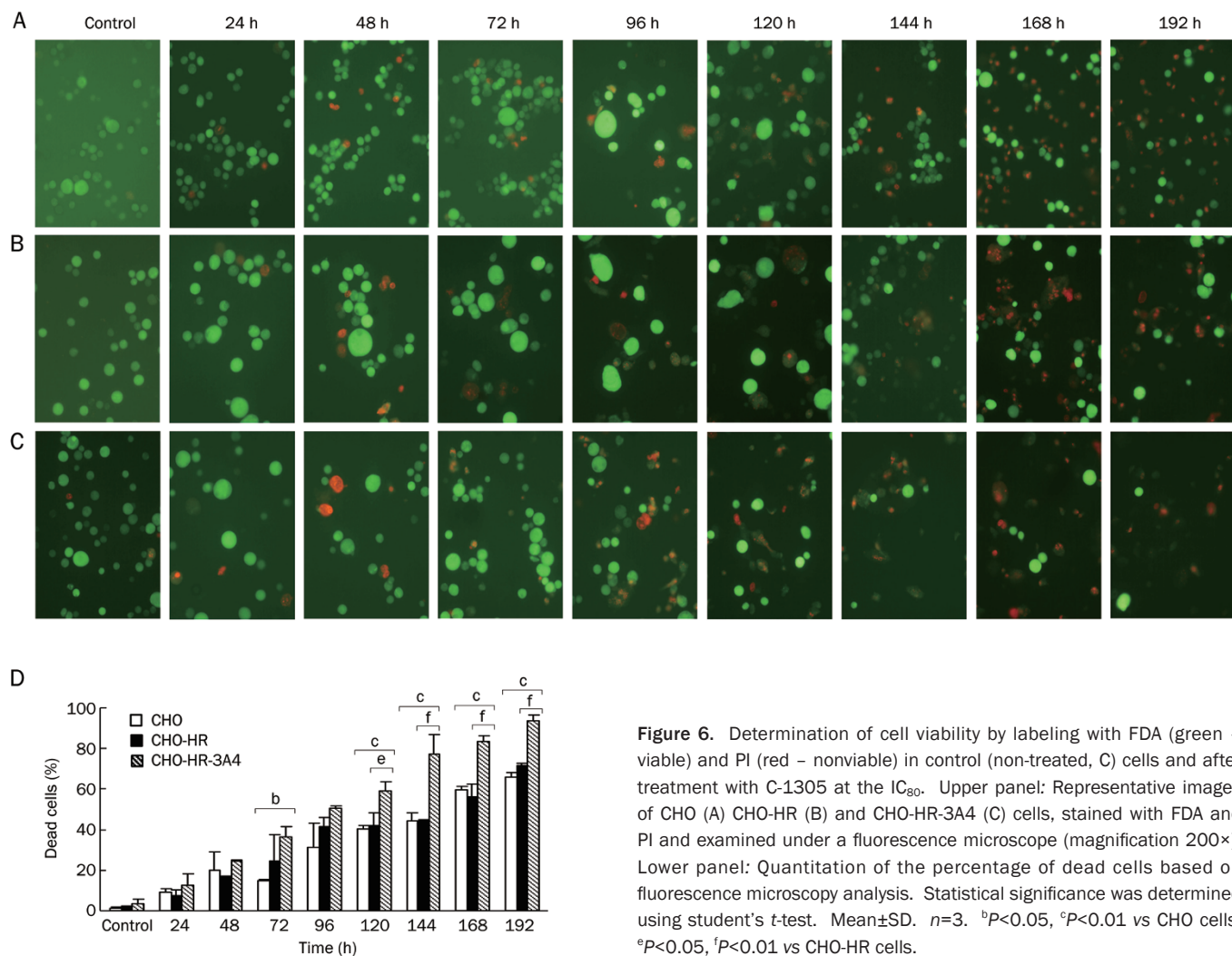
Figure 6. Determination of cell viability by labeling with FDA (green – viable) and PI (red – nonviable) in control (non-treated, C) cells and after treatment with C-1305 at the IC_{80}. Upper panel: Representative images of CHO (A) CHO-HR (B) and CHO-HR-3A4 (C) cells, stained with FDA and PI and examined under a fluorescence microscope (magnification 200×). Lower panel: Quantitation of the percentage of dead cells based on fluorescence microscopy analysis. Statistical significance was determined using student's *t*-test. Mean±SD. *n*=3. [b]$P<0.05$, [c]$P<0.01$ *vs* CHO cells. [e]$P<0.05$, [f]$P<0.01$ *vs* CHO-HR cells.

The results showed that the overexpression of human P450 reductase increased the cytotoxicity of C-1305 compared to wild-type cells, whereas overexpression of the CYP3A4 isoenzyme slightly reduced the cytotoxic action of the studied drug in comparison to CHO-HR cells. These results suggest that increased levels of cytochrome P450 reductase enhance the efficiency of this metabolic system, whereas dual expression of the CYP3A4 isoenzyme and cytochrome P450 reductase slightly decreases it. It is possible that the lower sensitivity of CHO-HR-3A4 cells to C-1305 compared with CHO-HR cells might result from the inhibitory properties of C-1305, which were demonstrated through recombinant and microsomal CYP3A4 expression in our previous studies[14]. Other antitumor agents, such as vincristine and vinblastine, demonstrate significantly lower cytotoxicities in CHO cells that overexpress CYP3A4 than in wild-type CHO cells[35]. In contrast, considerably increased doxorubicin activity has been observed in CHO cells with high CYP3A4 levels[36]; however, other studies gave contradictory results[37]. In turn, mitomycin C exhibits similar cytotoxicity in CHO cells overexpressing cytochrome P450 reductase and in wild-type CHO cells[38]. The above results,

including our findings for the triazoloacridinone C-1305, depend on the role of CYP3A4 metabolism in determining the final biological effects. When CYP3A4 metabolism leads to drug activation, then overexpression of this enzyme results in higher effectiveness. In contrast, participation of CYP3A4 in detoxification pathways results in a lower cytotoxicity for the drug. Alternatively, these inter-relations are more complicated when the therapeutic agent is able to interact with enzymatic proteins by physicochemical or covalent binding. As a result of such interactions, the induction or inhibition of CYP3A4 activity is observed. This mechanism appears to have taken place in the case studied here of the antitumor triazoloacridinone derivative C-1305.

Taking into account that C-1305 has a strong effect on the cell cycle of both cancer cells[13], wild-type cells and non-transformed cells[9], in the next part of the present study, we showed that this drug also has an impact on cell cycle progression in CHO cells that overexpress CYP3A4. After exposure to the drug for 24 h, CHO-HR and wild-type CHO cells were preferentially arrested in the G_2/M phase of the cell cycle, whereas CHO-HR-3A4 cells only slightly accumulated
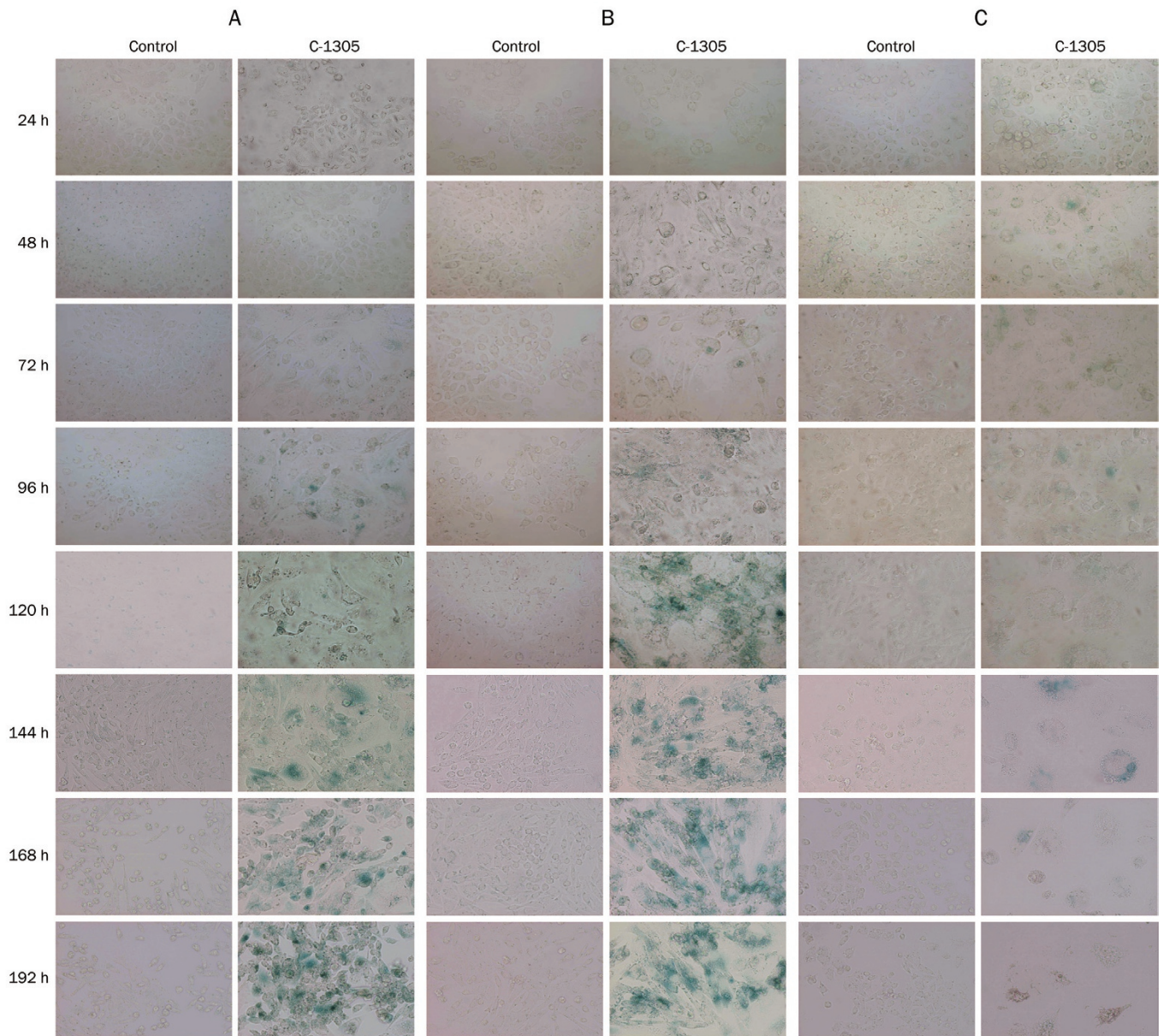
Figure 7. Assessment of cellular senescence induced by C-1305 treatment in CHO cells. Senescence-associated β-galactosidase (SA-β-Gal) staining (blue/green) in CHO (A), CHO-HR (B) and CHO-HR-3A4 (C) cells without treatment (control, C) or after treatment with C-1305 for the times indicated. The cells were photographed under a light microscope (magnification 200×).

in this phase. Moreover, a time-dependent increase in the sub-G_1 population of CHO cells (indicative of cells undergoing apoptosis) was also observed following C-1305 exposure. However, apoptotic DNA degradation was most prominent in CHO-HR-3A4 cells (72% of the population after 120 h of drug treatment).

To further explore the cellular effects induced by C-1305 in wild-type and CYP3A4-overexpressing CHO cells, morphological examination of the cells was performed. The cellular morphology of the CHO cells changed progressively with the increasing duration of C-1305 exposure. After 72 h of incubation with C-1305, characteristic apoptotic bodies and cells

with condensed nuclear chromatin were observed (Figure 3). Additionally, after prolonged drug incubation (120 h and longer), a small population of multinucleated CHO cells (wild-type and transfected), which is characteristic of mitotic death, was also identified. These morphological observations were verified by biochemical criteria typical for apoptosis, such as phosphatidylserine externalization and caspase-3 activation. Annexin V/PI staining revealed that approximately 50% of the CHO-HR cells were apoptotic after 120 h of incubation with C-1305. The populations of early and late apoptotic wild-type CHO and CHO-HR-3A4 cells reached approximately 32% and 37%, respectively, following 120 h of drug treatment. It is

worth noting that, beginning at 48 h, the population of necrotic wild-type CHO and CHO-HR cells (Annexin V⁻/PI⁺) significantly increased, at 96 h reached approximately 16%–20%, and after 120 h slightly decreased. In contrast, the population of necrotic CHO-HR-3A4 cells remained at the same level (~7% after 48–120 h). However, prolonged drug incubation (up to 192 h) resulted in massive detachment of the cells from the culture plates, suggesting that most of the cells were dead. FDA/PI dual staining demonstrated that the percentage of dead cells (PI-positive) reached 65% in wild-type CHO cells, 71% in CHO-HR cells and 93% in CHO-HR-3A4 cells after 192 h of C-1305 treatment (Figure 6).

Accordingly, flow cytometry analysis of active capsase-3 confirmed that apoptosis was the main response of CHO cells to C-1305 treatment. This mode of cell death was caspase-dependent in the three studied CHO cell lines; however, this effect was most prominent in CHO-HR-3A4 cells that coexpressed human P450 reductase and CYP3A4 (Figure 5).

Next, we demonstrated that the wild-type CHO and CHO-HR cells that did not die by apoptosis or necrosis following C-1305 exposure were in a state of senescence based on altered their cell morphology and the appearance of increased senescence-associated β-galactosidase (SA-β-gal) activity relative to the control (Figures 7A and 7B). In contrast, few enlarged or SA-β-gal-positive CHO-HR-3A4 cells were observed after C-1305 treatment (Figure 7C).

In conclusion, our findings indicated that different expression levels of the CYP3A4 isoenzyme affected the cellular response induced by C-1305 in CHO cells. Apoptosis and (to a lesser extent) necrosis play major roles in the response of CHO cells to C-1305 exposure. Importantly, these cellular effects appeared more quickly and were more profound in CHO-HR and CHO-HR-3A4 cells than in wild-type CHO cells. Moreover, prolonged drug treatment led to the induction of senescence, which was detected in wild-type cells and cells overexpressing human P450 reductase. In contrast, CHO cells that coexpressed human P450 reductase and CYP3A4 did not undergo senescence and died principally through apoptosis and necrosis.

In summary, CHO cells overexpressing the CYP3A4 isoenzyme appear to be a good model system to study the interrelation between CYP3A4 overexpression and the final cellular response induced by potential anticancer drugs. Using this model system, we demonstrated for the first time that the cytotoxic activity and cellular effects induced in tumor cells by the anticancer triazoloacridinone C-1305 were affected by the different expression levels of metabolic enzymes. Our results can serve as a beginning for further studies on the role of cytochrome P450 overexpression in the cellular response of human tumor cells following C-1305 treatment. Moreover, these results can be applied in the rational design of antitumor therapy that is directed to individual patients based on differences in the expression levels of cytochrome P450 enzymes.

Acknowledgements

Author contribution

References

1 Murray GI, Taylor MC, McFadyen MCE, McKay JA, Greenlee WF, Burke MD, *et al*. Tumor-specific expression of cytochrome P450 CYP1B1. Cancer Res 1997; 57: 3026–31.

2 Mitra R, Guo Z, Milani M, Mesaros C, Rodriguez M, Nguyen J, *et al*. CYP3A4 mediates growth of estrogen receptor-positive breast cancer cells in part by inducing nuclear translocation of phospho-Stat3 through biosynthesis of (±)-14,15-Epoxyeicosatrienoic Acid (EET). J Biol Chem 2011; 286: 17543–59.

3 Brimer C, Dalton JT, Zhu Z, Schuetz J, Yasuda K, Vanin E, *et al*. Creation of polarized cells coexpressing CYP3A4, NADPH cytochrome p450 reductase and MDR1/p-glycoprotein. Pharm Res 2000; 17: 803–10.

4 Chen L, Yu LJ, Waxman DJ. Potentation of cytochrome P450/cyclofosphamide-based cancer gene therapy by coexpression of the P450 reductase gene. Cancer Res 1997; 57: 4830–37.

5 Ding S, Yao D, Burchell B, Wolf CR, Friedberg T. High levels of recombinant CYP3A4 expression in Chinese hamster ovary cells are modulated by coexpressed human P450 reductase and hemin supplementation. Arch Biochem Biophys 1997; 348: 403–10.

6 Chołody WM, Martelli S, Konopa J. 8-Substituted 5-((aminoalkyl)amino)-6H-v-triazolo(4,5,1-de)acridin-6-ones as potential anti-neoplastic agents. Synthesis and biological activity. J Med Chem 1990a; 33: 2852–6.

7 Kuśnierczyk H, Chołody MW, Paradziej-Łukowicz J, Radzikowski C, Konopa J. Experimental antitumor activity and toxicity of the selected triazolo- and imidazoacridinones. Arch Immunol Ther Exp (Warsz) 1994; 42: 415–23.

8 Lemke K, Poindessous V, Składanowski A, Larsen AK. The antitumor triazoloacridinone C-1305 is a topoisomerase II poison with unusual properties. Mol Pharmacol 2004; 66: 1035–42.

9 Węsierska-Gądek J, Schloffer D, Gueorguieva M, Uhl M, Skladanowski A. Increased susceptibility of poly(ADP-ribose) polymerase-1 knockout cells to antitumor triazoloacridinone C-1305 is associated with permanent G₂ cell cycle arrest. Cancer Res 2004; 64: 4487–97.

10 Sabisz M, Węsierska-Gądek J, Składanowski A. Increased cytotoxicity of an unusual DNA topoisomerase II inhibitor compound C-1305 toward HeLa cells with downregulated PARP-1 activity results from re-activation of the p53 pathway and modulation of mitotic checkpoints. Biochem Pharmacol 2010; 79: 1387–97.

11 Lemke K, Wojciechowski M, Laine W, Bailly C, Colson P, Baginski M, *et al*. Induction of unique structural changes in guanine-rich DNA regions by the triazoloacridone C-1305, a topoisomerase II inhibitor with antitumor activities. Nucl Acid Res 2005; 33: 6034–47.

12 Koba M, Konopa J. Interactions of antitumor triazoloacridinones with DNA. Acta Biochim Pol 2007; 54: 297-306.

13 Augustin E, Moś-Rompa A, Skwarska A, Witkowski J, Konopa J.

Induction of G$_2$/M arrest and apoptosis of human leukemia cells by potent triazoloacridinone C-1305. Biochem Pharmacol 2006; 72: 1668–79.

14 Fedejko-Kap B, Niemira M, Radominska-Pandya A, Mazerska Z. Flavin monooxygenases, FMO1 and FMO3, not cytochrome P450 isoenzymes, contribute to metabolism of antitumor triazoloacridinone, C-1305, in liver microsomes and HepG2 cells. Xenobiotica 2011; 41: 1044–55.

15 Dimri GP, Lee X, Basile G, Acosta M, Scott G, Roskelley C, *et al*. A biomarker that identifies senescent human cell in culture and aging skin *in vivo*. Proc Natl Acad Sci U S A 1995; 92: 9363–7.

16 Earnshaw WC, Martins LM, Kaufmann SH. Mammalian caspases: structure, activation, substrates, and function during apoptosis. Annu Rev Biochem 1999; 68: 383-424.

17 Jones KH, Senft JA. An improved method to determine cell viability by simultaneous staining with Fluorescein Diacetate - Propidium Iodide. J Histochem Cytochem 1985; 33: 77–9.

18 Chang BD, Broude EV, Dokmanovic M, Zhu H, Ruth A, Xuan Y, *et al*. A senescence-like phenotype distinguishes tumor cells that undergo terminal proliferation arrest after exposure to anticancer agents. Cancer Res 1999; 59: 3761–7.

19 Kumar GN, Surapaneni S. Role of drug metabolism in drug discovery and development. Med Res Rev 2001; 21: 397–411.

20 Gonzales FJ, Gelboin HV. Role of human cytochrome P450 in the metabolic activation of chemical carcinogens and toxins. Drug Metab Rev 1994; 26: 165–83.

21 Guengerich FP. Roles of cytochrome P450 enzymes in chemical carcinogenesis and cancer chemotherapy. Cancer Res 1988; 48: 2946–54.

22 Guengerich FP. Metabolic activation of carcinogens. Pharmacol Ther 1992; 54: 17–62.

23 Kivisto KT, Kroemer HK, Eichelbaum M. The role of human cytochrome P450 enzymes in the metabolism of anticancer agents: implications for drug interactions. Br J Clin Pharmacol 1995; 40: 523–30.

24 Guengerich FP. Cytochrome P450 3A4: regulation and role in drug metabolism. Annu Rev Pharmacol Toxicol 1999; 139: 1–17.

25 Albin N, Massad L, Toussaint C, Mathieu MC, Morizet J, Parise O, *et al*. Main drug-metabolizing enzyme systems in human breast tumors and peritumoral tissues. Cancer Res 1993; 53: 3541–6.

26 Czerwinski M, McLemore TL, Gelboin HV. Quantification of CYP2B7, CYP4B1 and CYPOR messenger RNAs in normal human lung and lung tumors. Cancer Res 1994; 54: 1085–91.

27 Mekhail-Ishak K, Hudson N, Ming-Sound T, Batist G. Implications for therapy of drug-metabolizing enzymes in human colon cancer. Cancer Res 1989; 49: 4866–9.

28 Goetz MP, Knox SK, Suman VJ, Rae JM, Safgren SL, Ames MM, *et al*. The impact of cytochrome P450 2D6 metabolism in women receiving adjuvant tamoxifen. Breast Cancer Res Treat 2007; 101: 113–21.

29 Poljakova J, Eckschlager T, Hrabeta J, Hrebeckova J, Smutny S, Frei E, *et al*. The mechanism of cytotoxicity and DANN adduct formation by the anticancer ellipticine in human neuroblastoma cells. Biochem Pharmacol 2009; 77: 1466–79.

30 Wang Y, Gray JP, Mishin V, Heck DE, Laskin DL, Laskin JD. Distinct roles of cytochrome P450 reductase in Mitomycin C redox cycling and cytotoxicity. Mol Cancer Ther 2010; 9: 1852–63.

31 Lv X, Wan J, Yang J, Cheng H, Li Y, Ao Y, *et al*. Cytochrome P450 ω-hydroxylase inhibition reduces cardiomyocyte apoptosis via activation of ERK1/2 signaling in rat myocardial ischemia-reperfusion. Eur J Pharmacol 2008; 596: 118–26.

32 Holowkia A, Braszko J. Tamoxifen cytotoxicity in hepatoblastoma cells stably transfected with human CYP3A4. Biochem Pharmacol 2004; 67: 1057–64.

33 Donato MT, Lahoz A, Castell JV, Gomez-Lechon MJ. Cell lines: a tool for *in vitro* drug metabolism studies. Curr Drug Metab 2008; 9: 1–11.

34 Sharma SV, Haber DA, Settleman J. Cell line-based platforms to evaluate the therapeutic efficacy of candidate anticancer agents. Nat Rev Cancer 2010; 10: 803–10.

35 Yao D, Ding S, Burchell B, Wolf R, Friedberg T. Detoxication of Vinca alkaloids by human P450 CYP3A4-mediated metabolism; implications for the development of drug resistance. J Pharmacol Exp Ther 2000; 294: 387–95.

36 Lu H, Waxman DJ. Antitumor activity of methoxymorpholinyl Doxorubicin: potentation by cytochrome P450 3A metabolism. Mol Pharmacol 2005; 67: 212–9.

37 Rodriguez-Antona C, Leskela S, Zajac M, Cuadros M, Alves J, Moneo MV, *et al*. Expression of CYP3A4 as a predictor of response to chemotherapy in peripheral T-cell lymphomas. Blood 2007; 110: 3345-51.

38 Wang YJ, Yu CF, Chen LC, Chen CH, Lin JK, Liang YC, *et al*. Ketoconazole potentiates terfenadine-induced apoptosis in human HepG2 cells through inhibition of cytochrome P450 3A4 activity. J Cell Biochem 2002; 87: 147–59.